Biosensors and Bioelectronics 103 (2018) 94–98

Contents lists available at ScienceDirect

Biosensors and Bioelectronics

journal homepage: www.elsevier.com/locate/bios

Label-free impedimetric glycan biosensor for quantitative evaluation interactions between pathogenic bacteria and mannose

Feiyun Cui[a,b,d], Yi Xu[b,c,d,e,*], Renjie Wang[a,b,d], Haitao Liu[b,c], Li Chen[b,c,d,e,*], Qing Zhang[f], Xiaojing Mu[b,c,d,e]

[a] School of Chemistry and Chemical Engineering, Chongqing University, Chongqing 400030, China
[b] Key Disciplines Lab of Novel Micro-nano Devices and System Technology, Chongqing University, Chongqing 400030, China
[c] Key Laboratory for Optoelectronic Technology & System of Ministry of Education, Chongqing University, Chongqing 400044, China
[d] International R & D center of Micro-nano Systems and New Materials Technology, Chongqing University, Chongqing 400030, China
[e] School of Optoelectronics Engineering, Chongqing University, Chongqing 400044, China
[f] Chongqing institute for food and drug control, Chongqing 400044, China

ARTICLE INFO

Keywords:
Electrochemical impedance spectroscopy(EIS)
Glycan biosensor
Interactions between bacteria and glycan
Bacteria detection

ABSTRACT

In order to understanding the pathogenic mechanism of infectious diseases, it was important to study the selective recognition and interaction between pathogenic bacteria and host cells. In this paper, a novel electrochemical impedance biosensor was proposed, in which the Man/MUA-MH/Au sensing surface (Man: mannose; MUA: 11-mercapto eleven acid; MH: 6-mercapto hexanol) was fabricated and was of good biologically active and stability. The capture capacity of the designed sensing surface for *S. typhimurium* ATCC14028, *E. coli* JM109 and *E. coli* DH5α were characterized by Electrochemical impedance spectroscopy (EIS). According to Randless equivalent circuit and the Frumkin isotherm model, electron transfer impedance (R_{et}) was obtained and the binding affinity of the three bacteria and Man was calculated. It was shown that the sensing surface had a better binding affinity for *S. typhimurium* ATCC14028 with $K_{ADS(S.T.)} = 2.16 \times 10^6$ CFU/mL. The impedance normalized value NIC $_{(S.T.-Man)}$ was of a good linear relationship with the logarithm of bacterial concentration ($R^2 = 0.96$) in the range of 50–1000 CFU/mL. The detection limit was 50 CFU/mL. Meanwhile, the *E. coli* JM109 which expresses type 1 fimbriae was also adsorbed on the designed sensing surface with $K_{ADS(JM109)} = 5.84 \times 10^3$ CFU/mL. It was illustrated that the novel electrochemical impedance biosensor could be more rapid and reliable for studying interactions between pathogen and glycan, and it was also perspective for a new point-of-care diagnostic tool for evaluating the pathogenicity bacteria.

1. Introduction

Adhesion of pathogenic bacteria is a prerequisite for a majority of infectious diseases. A common way to activate adhesion is a specific recognition between bacteria and glycan on the surface of the host cells. Therefore, research on bacteria-glycan interactions is beneficial to further understand the pathogenic mechanism of infectious diseases. Meanwhile, it can provide new strategies for treatment of infectious diseases (Ielasi et al., 2016; Pera and Pieters, 2014; Spaulding et al., 2017). However, the current methods for researching pathogenic bacteria-glycan interactions were limited to optical microscopy and fluorescence spectroscopy. The optical microscopy was used to calculated dissociation constants of *E. coli* ORN178 (specifically expressed wild type 1 fimbriae) and mannose (Zhu et al., 2009). Their method has the advantages of less dosage of samples and high throughput, but the operation is time consuming and complicated. CdS@CTS (CTS: chitosan) quantum dots were synthesized based on the chemical similarity of the chitosan and the bacteria membranes (Abdelhamid and Wu, 2013). the binding constant between CdS@CTS and two kinds of bacteria were calculated by using the fluorescence spectroscopy, the values for both bacteria were all in the order of $10^5\,M^{-1}$. However, this method needs fluorescent label of glycan molecules, which may affect the biological activity of glycan molecules and pathogens, and then affect the detection results.

Electrochemical impedance spectroscopy (EIS) has advantages of sensitive, rapid and label-free, which has been considered as one of the most promising methods to study the interactions of biological particles (Bahadir and Sezginturk, 2016; Hushegyi et al., 2016; Lindholm-Sethson et al., 2010). Bacteria or cells specifically binding to the bioactive molecules which were fixed on the working electrode surface

* Corresponding authors at: Key Disciplines Lab of Novel Micro-nano Devices and System Technology, Chongqing University, Chongqing 400030, China.
E-mail addresses: xuyibbd@sina.com (Y. Xu), cl2009@cqu.edu.cn (L. Chen).

https://doi.org/10.1016/j.bios.2017.11.068
Received 24 August 2017; Received in revised form 9 November 2017; Accepted 29 November 2017
Available online 02 December 2017
0956-5663/

would affect the electrochemical polarization process, and slow down electron transfer rate significantly. By measuring the electron transfer impedance (R_{et}) and the electrical double layer capacitance (C_{dl}) of the surface, the interactions process and dynamics mechanism of biological particles can be analyzed. Faraday impedance method was firstly used by Kharitonov et al. (2000) to study the interactions between enzyme and the corresponding biological molecules, and the binding affinity of cytochrome oxidase and cytochrome c was calculated by using Benesi-Hildebrand equation. It has been proved that the impedance method can be used to quantitatively study the interaction of biomolecules on the electrode surface. In addition, the interactions between transcription factors and the corresponding dsDNA were studied by Xu et al. (2011) and Tersch and Lisdat (2011) through developing an impedance protein biosensor and an impedance DNA biosensor. All these studies illustrated that the impedance method was simple, sensitive, rapid and reproducible for studying the interactions of biological particles. The hemagglutinin of influenza virus was detected by Tkac et.al (Hushegyi et al., 2015) using impedance glycan biosensor, whose detection limit was down to aM magnitude. It was indicated that the impedance glycan biosensor was of high enough sensitivity. The specific recognition between *E. coli* and mannose was used by Guo et al. (2012) to quantitatively detect *E. coli* ORN 178, and the detection limit was 10^2 CFU/mL. The adsorption information of bacteria on the glycan surface can be obtained rapidly without labeling pathogens or glycan. However, to the best of our knowledge, the impedance based method has not been developed for studying the selective recognition between pathogenic bacteria and glycan.

Escherichia coli and *Salmonella* are two kinds of intestinal and bladder pathogens. *E. coli* (Type1) which express type 1 fimbriae can be selectively anchor on the mannan (Manα3Manα6Man) of the bladder tissue surface (Imberty and Varrot, 2008; Liu, 2008). *Salmonella typhimurium* and *Salmonella enteritidis* can selectively recognize mannose on the surface of the intestine, which can cause intestinal disease (Ohlsen et al., 2009). As mentioned above, a Man/MUA-MH/Au biosensor surface was proposed and prepared by immobilizing phenyl modified mannose molecules on the gold electrode surface which was modified by a self-assembly monolayer composed of 11-mercaptoalkanoic acid and 6-mercapto hexanol. Simultaneously, a new method based on impedimetric biosensor was established to study the selective recognition happened between *E. coli*, *Salmonella* and mannose. The recognition of *S. typhimurium* ATCC14028, *E. coli* JM109 and *E. coli* DH5α on the sensing surface were characterized by EIS. The corresponding electron transfer impedance (R_{et}) and binding affinities of the three bacteria and Man were calculated by using Randless equivalent circuit model and Frumkin isotherm model.

2. Experimental section

2.1. Materials, reagents and bacterial culture

The list of all materials and reagents employed in this work is mentioned in SI-1.1 (Supplementary Information 1.1). Experimental steps for bacterial culture are given in SI-1.2.

2.2. Preparation of Man/MUA-MH/Au

After the cleaning process, the electrodes were incubated with 1 mM solution of thiols (mixtures of 11-mercaptoundecanoic acid and 6-mercapto hexanol at ratio of 1:20, if not specified) as described previously (Hushegyi et al., 2015) for 14 h in dark at room temperature. The 1 mM stock solution of 11-MUA and 6-MH was prepared in ultrapure ethanol and stored at − 20 °C until use. After incubation, the electrodes were washed with ultrapure water and ethanol. Carboxyl groups on self-assembled monolayers(SAMs) layer were activated with 100 μl of 200 mM EDC and 50 mM NHS at ratio of 1:1 (solutions of EDC and NHS were prepared in ultrapure water and stored at − 20 °C in aliquots) for 20 min. After activation, the electrodes were washed with ultrapure water, and 2 mg/mL amino terminated glycan was reacted with the biosensor surface (glycan was dissolved in ultrapure water and stored at 4 °C in aliquots) at room temperature for 3 h to complete the glycan immobilization.

2.3. Characterization of Man/MUA-MH/Au stability and bacterial detection by EIS

Immersed the Man/MUA-MH/Au in a series of bacterial samples with different concentrations: 10 CFU/mL、50 CFU/mL、1×10^2 CFU/mL、5×10^2 CFU/mL、1×10^3 CFU/mL、5×10^3 CFU/mL、1×10^4 CFU/mL、5×10^4 CFU/mL、1×10^5 CFU/mL、5×10^6 CFU/mL、1×10^6CFU/mL. Rinse the electrode surface with ultrapure water after incubating it at 25 ℃ for 1 h, and then EIS measurements were performed.

EIS measurements were carried out with a three electrodes system, a saturated calomel electrode(SCE) as reference electrode, a gold working electrode, and a platinum counter electrode. EIS was measured with the Electrochemical System of a PARSTAT V3 (Princeton Co., USA). EIS was run in a single-compartment three electrode glass cell containing 15 mL of 1 M KCl and 2 mM $K_3[Fe(CN)_6]/K_4[Fe(CN)_6]$ (1:1 mixture). Impedance measurements were measured at an open circuit potential (OCP) to the SCE, and an alternating potential with a 5 mV amplitude was applied in the frequency range from 1 Hz to 100 kHz. All electrochemical measurements were performed in a Faraday cage.

2.4. Statistical analysis

The means ± standard deviations of three different electrodes with same experiment processing were calculated using Excel 2016 software. The statistical differences were determined with single-factor analysis of variance (one-way ANOVA) using Excel 2016 software (Xu et al., 2016). The significance level was set at a P value < 0.05.

3. Results and discussion

3.1. Characterization of Man/MUA-MH/Au

The construction process of Man/MUA-MH/Au and impedimetric biosensor based assay were outlined in Scheme SI-1. Cleanliness of the electrode is critical to ensure the uniformity, integrity and order of the self-assembled film, so the cleaning of the gold electrode is a key step for the successful construction of the biosensor surface. In this work, electron transfer impedance (R_{et}) of bare gold electrode was 40.17 ± 9.2 Ω after pretreatment of Gold Electrode (SI-1.3). R_{et} is the most sensitive component to characterize the sensing interface in Faraday electrochemical impedance spectroscopy. In our study, we choose the R_{et} of equivalent circuit (Scheme SI-2) as detection signal. After incubating the clean gold electrode in the mixed solution of 11-MUA and 6-MH for 14 h, a larger semicircle (Fig. 1A-b) appeared in the Nyquist plot that meant SAMs was formed on the surface of the electrode, and at this time the R_{et} was 1095 ± 94 Ω. Then the -COOH was activated by the mixed solution of EDC/NSH to make it into active ester group, the R_{et} was reduced to 427.3 ± 74 Ω here, which may be due to a decrease of the negative charge on SAM. After the amino glycoside was immobilized on the SAM by covalent bond, and R_{et} increased to 725.5 ± 97 Ω. The sensing surface was not stable in PBS until incubate for 12 h (3.2 section discussed in detail). At this point, the impedance of sensing surface was larger than which was just built (Fig. 1A-e). The stabile sensing surface was incubated with *S. typhimurium* ATCC14028 ($C = 1 \times 10^6$ CFU/mL) solution at RT for 1 h, and the R_{et} reached 2749 ± 219 Ω (Fig. 1A-f) which showed that the surface was of the capture capacity for *S. typhimurium* ATCC14028.

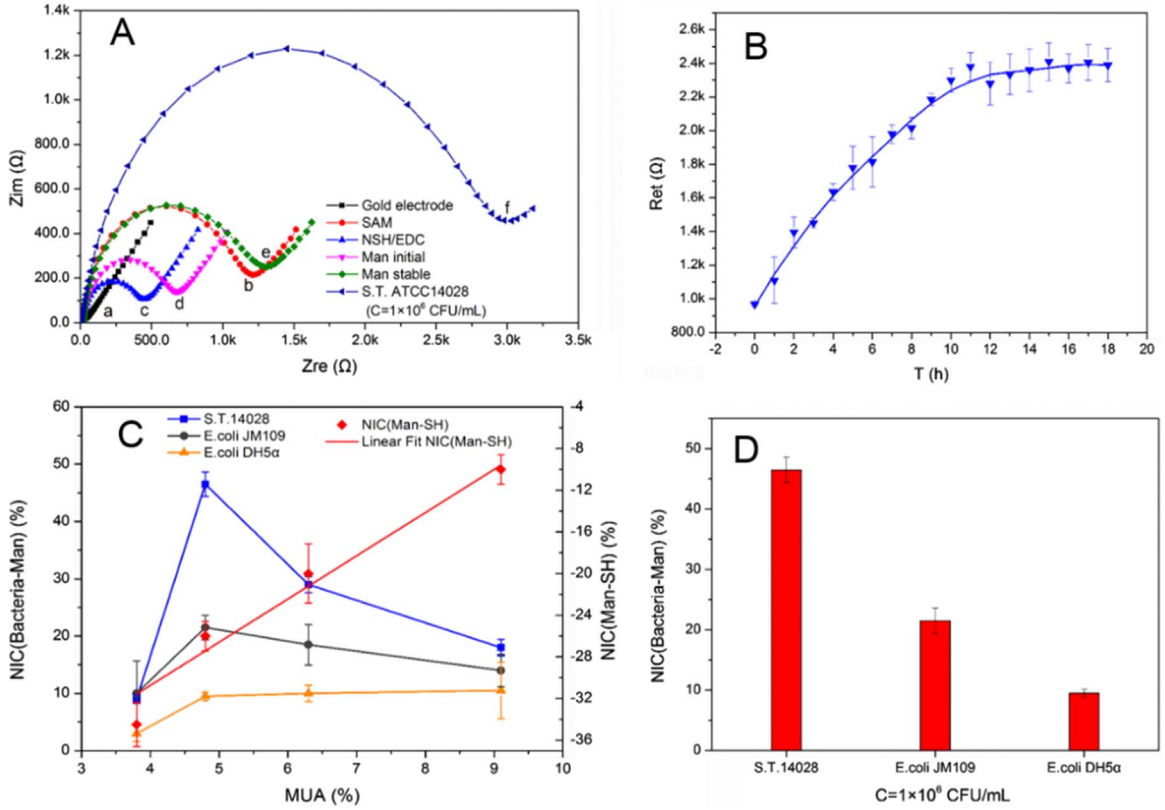

Fig. 1. (A) Impedance characterization of the build-up process of the Man/MUA-MH/Au with the formation of a mixed SAM composed of 11-meracptoundecanoic acid (11-MUA) and 6-mercapto hexanol (6-MH). (B) R_{et} changes of Man/MUA-MH/Au electrode when 11-MUA:6MH = 1:20 in PBS (n = 3). (C) Adsorption plot of three kinds of bacteria (C = 1 × 10^6 CFU/mL) under different ratios of 11-MUA and 6-MH (n = 3). (D) Selectivity plot for three kinds of bacteria of Man/MUA-MH/Au when 11-MUA:6MH = 1:20.

3.2. Stability test of Man/MUA-MH/Au

The sensing surface was not stable after the initial immobilized with the 4-Amino-phenyl α-D-Mannopyranoside. To avoid false-positive results in bacterial capture experiments, it was necessary to incubate the sensing surface in sterile PBS until stable. The sensing surface constructed in this paper was basically stable after 12 h, as was shown in Fig. 1B, the R_{et} value of the sensing surface was increased within 12 h, then it tended to be balanced, which may be mainly due to rearrangement and conformation changes of glycan molecules.

In addition to the conformational change of glycan molecules, the stability of sensing surface can be influenced by some other factors, such as UV light, temperature, the applied voltage, and even these factors could destroy the surface. Therefore, the temperature at every step was strictly controlled and UV irradiation was avoided.

$[Fe(CN)_6]^{3-/4-}$ is a kind of redox probe commonly used to characterize electron transfer (Lazar et al., 2016), however by comparing the testing values of repeated measurements for the same electrode, the R_{et} values is unstable in an electrolyte solution containing $[Fe(CN)_6]^{3-/4-}$, which seriously affect the sensitivity of the bacteria detection. In Guo's studies, PBS (pH = 7.2) containing 0.1 M $K_3[Fe(CN)_6]/K_4[Fe(CN)_6]$ (1:1 mixture) was applied as electrolyte solution, the electrodes modified with same SAMs had different initial impedances and final interfacial R_{et} values (1.6 kΩ to 30 kΩ). What's more, they took different time periods (5 h to 2 d) to reach equilibrium. This may be due to the excessive content of $K_3[Fe(CN)_6]$/ $K_4[Fe(CN)_6]$. When $[Fe(CN)_6]^{3-/4-}$ contacted with gold electrode through defects of SAMs, $Au(CN)^-$ would be formed and led to a corrosion of gold electrode, and then affected the stability of sensor surface. Bogomolova's studies showed that when the concentration of $K_3[Fe(CN)_6]$ and $K_4[Fe(CN)_6]$ was less than 2 mM, the unstable R_{et} changes could be significantly reduced (Bogomolova et al., 2009). Therefore, we chose 1 M KCl, 2 mM $K_3[Fe(CN)_6]$ and 2 mM $K_4[Fe(CN)_6]$ as electrolyte solution for impedance measurements.

3.3. Optimization of biological activity of Man/MUA-MH/Au

When the lectin of pathogen surface selectively recognized the glycan molecules, the glycan density dramatically could influence the strength and mode of interactions. A high glycan density on the sensing surface induced multivalent interactions, and on the contrary, monovalent interactions occurred under low glycan density conditions (Liang et al., 2007; Mammen et al., 1998; Muller et al., 2016; Zeng et al., 2016). However, the super high glycan density impeded the match between carbohydrate and lectins due to the presence of steric hindrance, which weakened the interaction between them (Yang et al., 2014, 2016).

In order to make sure the prepared sensing surface could interact with the pathogen effectively, 11-MUA was used as functional molecule to fix the 4-Amino-phenyl α-D-Mannopyranoside to the surface of the gold electrode, 6-MH was used to adjust the density of 11-MUA in this sensing surface. The normalized impedance change (NIC) of *S. typhimurium* ATCC14028, *E. coli* JM109 and *E. coli* DH5α were tested when the ratio of 11-MUA and 6-MH were 1:10(9.1%), 1:15(6.3%), 1:20(4.8%), 1:25(3.8%). The value of NIC was given by following formula (Varshney and Li, 2007):

$$NIC_{(Bacteria-Man)} = \frac{R_{et\,(Bacteria)} - R_{et\,(Man)}}{R_{et\,(Man)}} \times 100\% \quad (1)$$

where $NIC_{(Bacteria-Man)}$ is normalized impedance change of $R_{et\,(Bacteria)}$ to $R_{et\,(Man)}$, $R_{et\,(Man)}$ is electron transfer impedance for a control sample and $R_{et\,(Bacteria)}$ is the electron transfer impedance for a sample containing bacteria. An average of three readings and their standard deviation were calculated for each concentration of bacteria.

The results showed that the adsorption performance of Man/MUA-MH/Au for *S. typhimurium* ATCC14028 was the best when the concentration of MUA was 4.8% at 1:20, the $NIC_{(Bacteria\text{-}Man)}$ was 46.5%, and *E. coli* JM109 and DH5α were also reach the maximum value of 21.2% and 9.4% respectively (Fig. 1C). Micrograph of the Man sensing surface and its microscopic observations after incubation with 1 h in three bacteria confirmed the result (Fig. SI-1). It showed the Man/MUA-MH/Au has a selective recognition for both *S. typhimurium* ATCC14028 ($P = 0.0004$) and *E. coli* JM109 ($P = 0.01$), not for *E. coli* DH5α ($P = 0.09$). This was because both *S. typhimurium* ATCC14028 and *E. coli* JM109 express type 1 pili. In addition, the $NIC_{(Bacteria\text{-}Man)}$ of *S. typhimurium* ATCC14028 and *E. coli* JM109 were different, which indicated that the sensing surface can differentiate subtypes of the gram negative bacteria which express type 1 fimbriae (Fig. 1D).

It was also found that $NIC_{(Man\text{-}SH)}$ was proportional to $C_{11\text{-}MUA}$ as the percentage of 11-MUA increased (Fig. 1C, red line, right ordinate). $NIC_{(Man-SH)}$ is normalized impedance change of $R_{et(Man)}$ to $R_{et(NSH-EDC)}$, $R_{et(Man)}$ is electron transfer impedance when Man/MUA-MH/Au was stable. $R_{et(NSH-EDC)}$ is the electron transfer impedance when carboxyl groups on SAM layer were activated with EDC and NHS (Please refer to Scheme SI-1). The linear relationship is $NIC_{(Man\text{-}SH)} = 4.15[C_{11\text{-}MUA}] - 47$, $R^2 = 0.96$. It provides a new method for the quantitative determination of the glycan molecules on sensing surfaces.

3.4. Calculation of binding affinity between bacteria and mannose on the designed sensing surface

For a deeper understanding of the interaction between mannose and bacteria on the sensing surface, the isothermal adsorption model was used to establish the relationship between the coverage of bacteria θ and the concentration of bacteria $[C]$. According to Frumkin isotherm (Smith et al., 2003):

$$[C] = K_{ADS}^{-1}\frac{\theta}{1-\theta}e^{-2a\theta} \quad (2)$$

where K_{ADS} is the adsorption coefficient, which can be used to express the binding affinity of Man and bacteria. θ can be calculated by the electron transfer impedance:

$$\theta = \frac{\triangle R_{et}}{\triangle R_{etmax}} \quad (3)$$

$\triangle R_{et}$ is the difference of $R_{et\ (Bacteria)}$ and $R_{et\ (Man)}$ for a certain concentration of bacteria. $\triangle R_{etmax}$ is the difference between $R_{et\ (Bacteria)}$ and $R_{et\ (Man)}$ when the adsorbed bacteria reached saturation. By changing the bacteria concentration, a series of corresponding electron transfer impedance of bacterial adsorption were detected. Make the diagram of $[C]$ and θ.

Fig. 2A showed the capture of *S. typhimurium* ATCC14028 on the sensing surface. When the bacterial concentration was 1×10^5 CFU/mL, $R_{et(S.T.)}$ reached the maximum. According to the fitting result, $K_{ADS(S.T.)} = 2.16 \times 10^6$ CFU/mL, and the correlation coefficient was $R^2 = 0.96$. The adsorption of *E. coli* JM109 on the sensing surface was shown in Fig. 2B, when the bacterial concentration was 5×10^4 CFU/mL, $R_{et(JM109)}$ had the maximum value. According to the fitting result, $K_{ADS(JM109)} = 5.84 \times 10^3$ CFU/mL, and the correlation coefficient was $R^2 = 0.98$.

3.5. Detection of S. typhimurium ATCC14028

In order to verify the potential of the Man/MUA-MH/Au for

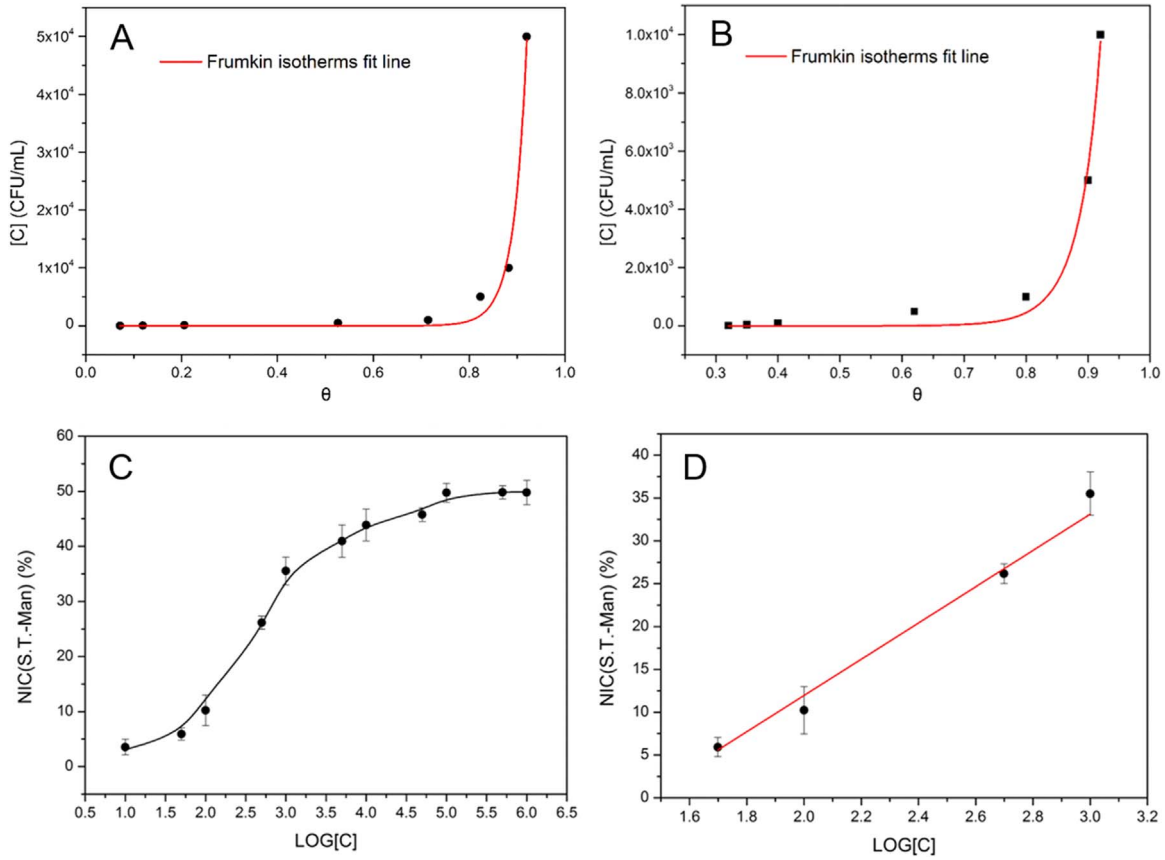

Fig. 2. Plots of bacteria surface coverage (fraction of occupied surface sites, θ) as a function of bacteria concentration in the solution. The data shown correspond to (A) the binding of *S. typhimurium* ATCC14028 and (B) the binding of *E. coli* JM109 to a mannose surface. The data have been fit to Frumkin isotherms (red lines). (C) Relationship between $NIC_{(S.T.\text{-}Man)}$ and *S. typhimurium* ATCC14028 concentrations; (D) Linear fitting with a logarithmic abscissa in a range of bacterial concentrations from 50 to 1000 CFU/mL.

Table 1
Comparison of EIS based label-free biosensors for *Salmonella* detection.

Biosensor	Pathogen	Nanomaterial	Linearity range CFU/mL	LOD CFU/mL	Reference
Immunosensor	*S. typhimurium*	MSNTs	10^3–10^7	5×10^2	(Nguyen et al., 2014)
Immunosensor	*S. typhimurium*			500	(Nandakumar et al., 2008)
Immunosensor	*S. typhimurium*	AuNPs MWCNTs	10^3–10^7	500/1000	(Dong et al., 2013)
Immnunosensor	*S. typhimurium*		10^3–10^8	10^3	(Farka et al., 2016)
Aptasensor	*S. typhimurium*		10^2–10^8	3	(Sheikhzadeh et al., 2016)
Aptasensor	*S.*ATCC 50761	rGO MWCNTs	75–7.5 $\times$ 10^5	25	(Jia et al., 2016)
Glycansensor	*Salmonella* ATC14028		50–10^3	50	This work

Nanomaterial is used in biosensors to magnify detection signals and enhance sensor sensitivity. MSNTs: magnetic silica nanotubes; AuNPs: Au nanomaterials; rGO: reduced Graphene oxide; SWCNTs: Single Walled Carbon nanotubes; LOD: limit of detection.

selective detection of *S.T.* ATCC14028, the relationship between $NIC_{(S.T.-Man)}$ and the logarithm of the concentration LOG[C] was analyzed (Fig. 2C). It showed that the $NIC_{(S.T.-Man)}$ increased with the increase of concentration of *S. typhimurium* ATCC14028 and the adsorption amount of bacteria on the sensing surface also increased until the concentration reached 1×10^5 CFU/mL. With the concentration of *S. typhimurium* ATCC14028 increased from 50 CFU/mL to 1000 CFU/mL, $NIC_{(S.T.-SH)}$ were directly proportional to the LOG[C] (Fig. 2D). The linear relationship was $NIC_{(S.T.-SH)} = 21.16\ \mathrm{LOG[C]} - 30.38$, and the correlation coefficient was $R^2 = 0.98$. The results showed that the limit of detection(LOD) for *S. typhimurium* ATCC14028 could reach 50 CFU/mL, which provided a basis for the subsequent selective detection of bacteria by glycan biosensor.

Detection of *S. typhimurium* in food has been reviewed (Silva et al., 2018). However, biosensors designed for the detection of *S. typhimurium* are mainly immunosensors and aptasensor, which could be costly and cumbersome. Despite the fact that our glycan-biosensor has higher LOD for *S. typhimurium* ATCC14028 compared to reported EIS based label-free aptasensors (Table 1), it provides a new strategy for the design of *S. typhimurium* detection sensors. Most importantly, we report the first electrochemical glycan biosensor designed for the detection of *S. typhimurium*. In addition, our biosensor performance is obtained with direct way without the amplification step.

4. Conclusions

A novel electrochemical impedance biosensor was proposed and constructed with a stable and biologically active Man/MUA-MH/Au sensing surface. The adsorption of *S. typhimurium* ATCC14028, *E. coli* JM109 and *E. coli* DH5α on the sensing surface was detected by EIS. The proposed sensing surface was of stronger adsorption ability for *S. typhimurium* ATCC14028 with the adsorption coefficient $K_{ADS(S.T.)}$ was 2.16×10^6 CFU/mL. A good linear relationship between the normalized value $NIC_{(S.T.-Man)}$ and the logarithm of the bacteria concentration with correlation coefficient $R^2 = 0.98$ in the range of 50–1000 CFU/mL was obtained, and the detection limit achieved 50 CFU/mL. Meanwhile, *E. coli* JM109 was also absorbed by the designed surface with adsorption coefficient K_{ADS} was 5.84×10^3 CFU/mL. The advantages of the proposed electrochemical impedance biosensor were fast, sensitive, simple and label-free. It was also shown great promise as a new point-of-care diagnostic tool for evaluating the pathogenicity of unknown bacteria.

Acknowledgments

The work described was supported by National Natural Science Foundation of China (No.21375156), High Technology Research and Development Program of China (Ministry of Science and Technology 863 Plan) (No.2015AA021104), Frontier Research Key Projects of Chongqing Science and Technology Committee (cstc2015jcyjBX0010), Scientific and Technical Innovation Projects for People's Livelihood of Chongqing Science and Technology Committee, (cstc2015shmszx00014).

Appendix A. Supporting information

Supplementary data associated with this article can be found in the online version at http://dx.doi.org/10.1016/j.bios.2017.11.068.

References

Abdelhamid, H.N., Wu, H.F., 2013. J. Mater. Chem. B 1 (44), 6094–6106.
Bahadir, E.B., Sezginturk, M.K., 2016. Artif. Cells Nanomed. Biotechnol. 44 (1), 248–262.
Bogomolova, A., Komarova, E., Reber, K., Gerasimov, T., Yavuz, O., Bhatt, S., Aldissi, M., 2009. Anal. Chem. 81 (10), 3944–3949.
Dong, J., Zhao, H., Xu, M., Ma, Q., Ai, S., 2013. Food Chem. 141 (3), 1980–1986.
Farka, Z., Jurík, T., Pastucha, M., Kovář, D., Lacina, K., Skládal, P., 2016. Electroanalysis 28 (8), 1803–1809.
Guo, X., Kulkarni, A., Doepke, A., Halsall, H.B., Iyer, S., Heineman, W.R., 2012. Anal. Chem. 84 (1), 241–246.
Hushegyi, A., Bertok, T., Damborsky, P., Katrlik, J., Tkac, J., 2015. Chem. Commun. 51 (35), 7474–7477.
Hushegyi, A., Pihikova, D., Bertok, T., Adam, V., Kizek, R., Tkac, J., 2016. Biosens. Bioelectron. 79, 644–649.
Ielasi, F.S., Alioscha-Perez, M., Donohue, D., Claes, S., Sahli, H., Schols, D., Willaert, R.G., 2016. mBio 7 (4), e00584–16.
Imberty, A., Varrot, A., 2008. Curr. Opin. Struct. Biol. 18 (5), 567–576.
Jia, F., Duan, N., Wu, S., Dai, R., Wang, Z., Li, X., 2016. Microchim. Acta 183 (1), 337–344.
Kharitonov, A.B., Alfonta, L., Katz, E., Willner, I., 2000. J. Electroanal. Chem. 487 (2), 133–141.
Lazar, J., Schnelting, C., Slavcheva, E., Schnakenberg, U., 2016. Anal. Chem. 88 (1), 682–687.
Liang, P.H., Wang, S.K., Wong, C.H., 2007. J. Am. Chem. Soc. 129 (36), 11177–11184.
Lindholm-Sethson, B., Nystrom, J., Malmsten, M., Ringstad, L., Nelson, A., Geladi, P., 2010. Anal. Bioanal. Chem. 398 (6), 2341–2349.
Liu, H., 2008. Pathogenic Bacterial Sensors Based on Carbohydrates as Sensing Elements. Springer, New York.
Mammen, M., Choi, S.K., Whitesides, G.M., 1998. Angew. Chem. Int. Ed. 37, 2754–2794.
Muller, C., Despras, G., Lindhorst, T.K., 2016. Chem. Soc. Rev. 45 (11), 3275–3302.
Nandakumar, V., La Belle, J.T., Reed, J., Shah, M., Cochran, D., Joshi, L., Alford, T.L., 2008. Biosens. Bioelectron. 24 (4), 1039–1042.
Nguyen, P.-D., Tran, T.B., Nguyen, D.T.X., Min, J., 2014. Sens. Actuators B 197, 314–320.
Ohlsen, K., Oelschlaeger, T.A., Hacker, J., Khan, A.S., 2009. Top. Curr. Chem. 288, 17–65.
Pera, N.P., Pieters, R.J., 2014. Med. Chem. Commun. 5 (8), 1027–1035.
Sheikhzadeh, E., Chamsaz, M., Turner, A.P.F., Jager, E.W.H., Beni, V., 2016. Biosens. Bioelectron. 80, 194–200.
Silva, N.F.D., Magalhães, J.M.C.S., Freire, C., Delerue-Matos, C., 2018. Biosens. Bioelectron. 99, 667–682.
Smith, E.A., Thomas, W.D., Kiessling, L.L., Corn, R.M., 2003. J. Am. Chem. Soc. 125 (20), 6140–6148.
Spaulding, C.N., Klein, R.D., Ruer, S., Kau, A.L., Schreiber, H.L., Cusumano, Z.T., Dodson, K.W., Pinkner, J.S., Fremont, D.H., Janetka, J.W., Remaut, H., Gordon, J.I., Hultgren, S.J., 2017. Nature 546 (7659), 528–532.
Tersch, C., Lisdat, F., 2011. Electrochim. Acta 56 (22), 7673–7679.
Varshney, M., Li, Y., 2007. Biosens. Bioelectron. 22 (11), 2408–2414.
Xu, J., He, X., Jin, L., Jiang, L., Zhou, Y., Kang, Z., Peng, R., Lee, S.-T., 2011. Electrochim. Acta 56 (16), 5759–5765.
Xu, M., Wang, R., Li, Y., 2016. Talanta 148, 200–208.
Yang, J., Chazalviel, J.-N., Siriwardena, A., Boukherroub, R., Ozanam, F., Szunerits, S., Gouget-Laemmel, A.C., 2014. Anal. Chem. 86 (20), 10340–10349.
Yang, J., Siriwardena, A., Boukherroub, R., Ozanam, F., Szunerits, S., Gouget-Laemmel, A.C., 2016. J. Colloid Interface Sci. 464, 198–205.
Zeng, X., Qu, K., Rehman, A., 2016. Acc. Chem. Res. 49 (9), 1624–1633.
Zhu, X.Y., Holtz, B., Wang, Y., Wang, L.-X., Orndorff, P.E., Guo, A., 2009. J. Am. Chem. Soc. 131 (38), 13646–13650.